MODELLING OF IRRIGATION WATER REQUIREMENT FOR WHEAT UNDER SUB-TROPICAL MONSOON CLIMATE IN NORTH-CENTRAL BANGLADESH

Md Feroz Miah[1*], Md. Afzal Hossain[2], Iqbal Hossain Imon[3], Nahid Hassan Suzan[4], Md Ruhul Amin Hira[5], Dr. Md. Touhidul Islam[6]

[1] *Graduate Student, Mymensingh Engineering College, Mymensingh, Bangladesh, e-mail:* ferozmiah.mec@gmail.com
[2] *Graduate Student, Mymensingh Engineering College, Mymensingh, Bangladesh, e-mail: mdafzalhossain672@gmail.com*
[3] *Graduate Student, Mymensingh Engineering College, Mymensingh, Bangladesh, e-mail: imonhasan971@gmail.com*
[4]*Graduate Student, Mymensingh Engineering College, Mymensingh, Bangladesh e-mail:* nahidhassansuzan@gmail.com
[5]*Graduate Student, Mymensingh Engineering College, Mymensingh, Bangladesh, e-mail:* hiraruhulamin529@gmail.com
[6]*Associate Professor, Bangladesh Agricultural University, Mymensingh, Bangladesh, e-mail: touhidul.iwm@bau.edu.bd*

***Corresponding Author**

ABSTRACT

By comparing baseline climate conditions with future projections for the 2040s and 2070s under RCP4.5 and RCP8.5, this study explores the anticipated effects of climate change on wheat water demand and irrigation requirements in Mymensingh, Bangladesh. We calculated reference evapotranspiration (ETo) using the FAO Penman Monteith method using downscaled climate model outputs. We then combined ETo with crop coefficients (Kc) and effective rainfall (ER) to determine the potential irrigation requirement (PIR) and crop water requirement (PCWR) for the wheat-growing season. The findings show that maximum (Tmax) and minimum (Tmin) temperatures will consistently rise in all future scenarios, with greater increases under RCP8.5 and in the 2070s. While effective rainfall decreases in most scenarios (up to −19.0%), ETo increases significantly, roughly +14.9% (RCP4.5, 2040s) to +25.4% (RCP8.5, 2070s). While effective rainfall decreases in most scenarios (up to −19.0% in RCP8.5, 2040s), ETo increases significantly, roughly +14.9% (RCP4.5, 2040s) to +25.4% (RCP8.5, 2070s). As a result, PCWR and PIR rise in comparison to the baseline, while PIR values stay at or above current levels. Increased irrigation dependence, increased pressure on surface and groundwater resources, and an increased risk of yield losses if adaptation is not implemented are all implied by the combined trends, which indicate increased evaporative demand and decreased natural water supply during crucial crop stages. To manage agricultural water sustainably under future climates, we advise giving priority to climate-smart irrigation, varietal and planting-date adjustments, better water storage techniques, and policy measures.

Keywords: *Wheat, Water Requirements, MarkSim GCM, CROPWAT, RCPs, Bias Correction.*

1. INTRODUCTION

Global temperature and precipitation patterns are changing due to climate change, which has important ramifications for agricultural water demand and food security. Wheat is still a major winter (rabi) crop in South Asia, particularly in Bangladesh. Its success is dependent on the amount and timing of water availability during critical phenological stages (emergence, vegetative growth, anthesis, and grain filling). Crop water requirements and irrigation needs can be changed by changes in monthly rainfall distribution, variations in maximum and minimum temperatures (Tmax, Tmin), and rising atmospheric evaporative demand. Designing successful adaptation strategies that ensure yields while preserving water resources requires an understanding of these changes on a local level. For the wheat-growing season in Mymensingh, this study evaluates anticipated changes in Tmax, Tmin, precipitation, ETo, effective rainfall (ER), potential crop water requirement (PCWR), and potential irrigation requirement (PIR). We contrast future projections for the 2040s and 2070s under two greenhouse-gas concentration pathways, RCP4.5 and RCP8.5, with a recent baseline. Crop coefficients and basic effective-rainfall methods are used to estimate seasonal PCWR and PIR, and climate-model-derived inputs are used to compute ETo using the FAO Penman Monteith equation. In the context of Mymensingh, the goals are to: quantify the direction and magnitude of climate-driven changes in the thermal and moisture drivers of wheat water demand; investigate how these changes translate into shifts in irrigation requirements; and discuss implications for water resources and on-farm adaptation. The study highlights where and when interventions will be most important to maintain wheat productivity under a warmer and, in many cases, drier future by integrating climatic and crop-hydrological metrics. This information is useful for water managers, extension services, and farmers in the area.

2. METHODOLOGY

Figure 1 shows the methodology of this work.

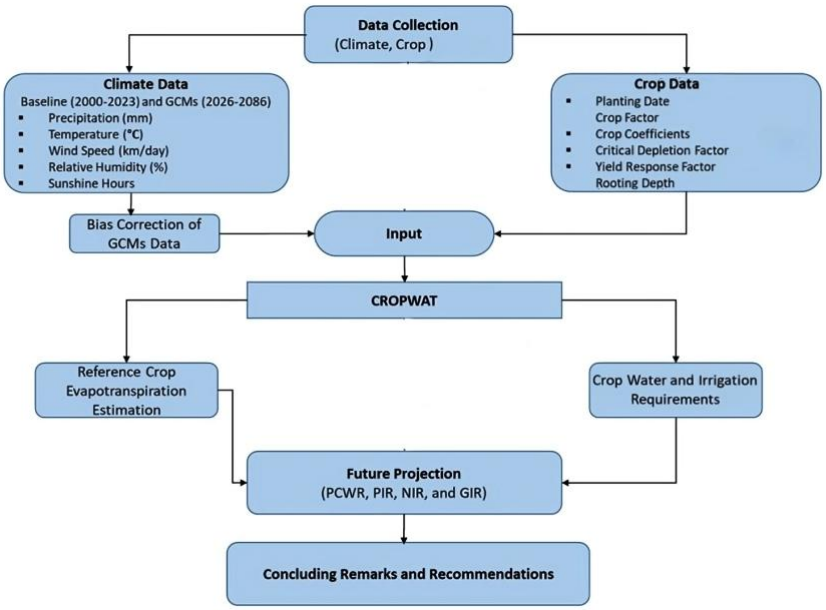

Fig. 1. Flow diagram.

2.1 Study Area

One of the most productive agricultural areas in north-central Bangladesh, the Mymensingh district, was the site of the study. This district has a humid subtropical climate with monsoon influences that create two distinct seasons: dry and wet. It is located between latitudes 24° 15′ N and 25° 10′ N and longitudes 90° 15 ′ E and 90° 45 ′ E. The study area's geographical features are shown in Fig. 2. Agriculture, particularly the production of rice, wheat, and other crops, makes up the majority of the

LULC. The region's soil is mostly loamy, with a moderate capacity for water retention and drainage. For wheat farming, this is crucial.

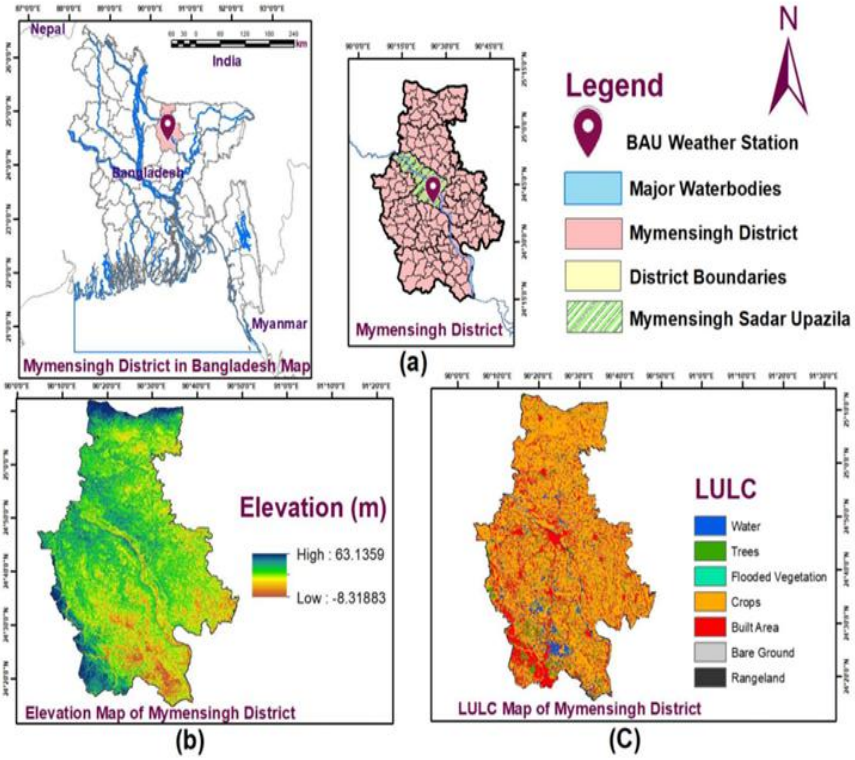

Fig. 2. Map of the study area depicting (a) the weather station located near Bangladesh Agricultural University (BAU) in Mymensingh, Bangladesh, (b) the elevation profile, and (c) the land use and land cover (LULC) map of the Mymensingh district.

2.2 Data Collection

The on-site weather station close to Bangladesh Agricultural University (BAU) in Mymensingh, Bangladesh, provided historical climate data, including minimum and maximum temperatures and rainfall. The dataset covers the years 2000 through 2023. This dataset's continuity test revealed a few missing observations: Averages from nearby days were used to interpolate missing values for short intervals (one to three days). As per established methodologies, averages from corresponding days in nearby years were used for longer gaps (greater than three days). The data was cross-checked with observations from another nearby weather station to confirm the records' accuracy and consistency. The Bangladesh Agricultural Research Institute (BARI) provided crop-specific wheat parameters.

2.3 General Circulation Models and Bias Corrections

Three reputable and well-known GCMs were used in this study to project future climate scenarios: BCC-CSM1-1-M and MIROC5. The Beijing Climate Center (BCC) created the BCC-CSM1-1-M model, which offers a thorough simulation of global climate behavior (Wu et al., 2014). The Japan Agency for Marine-Earth Science and Technology, the National Institute for Environmental Studies, and the University of Tokyo collaborated to create the MIROC5 model, which provides simulations of future climate dynamics based on coupled atmosphere-ocean interactions (Watanabe et al., 2010). Based on two RCPs, RCP 4.5 and RCP 8.5, the study created climate projections. Since the GCMs did not provide relative humidity projections, CROPWAT modeling assumed that relative humidity would stay constant for the future scenarios based on baseline conditions. Statistical downscaling techniques were used to address the inherent uncertainties of GCMs at regional scales. These methods ensure a more accurate depiction of local climate conditions by refining the broad-scale outputs of GCMs into finer, more region-specific projections. Because linear scaling can effectively address systematic biases in climate model outputs, it was chosen as the bias correction method in this study. This method is

especially useful for variables like temperature and precipitation because it modifies the mean of model-projected values to match observed historical data (Teutschbein & Seibert, 2012).

2.4 Performance Evaluation of Selected General Circulation Models

The referenced historical weather station data will be used to compare the performance of the two chosen climate models using RCP 4.5 and RCP 8.5. The performance analysis concentrated on the years 2007 to 2023, in line with the RCPs' data initiation in 2006, even though the baseline data from 2000 to 2023 was available. Because they are robust in capturing different aspects of model accuracy, key statistical indices such as coefficient of determination (R^2), Nash-Sutcliffe efficiency (NSE), percent bias (PBIAS), and mean absolute error (MAE) will be used. PBIAS values within 35 indicate satisfactory model performance (Lamichhane et al., 2024), while R^2 and NSE show the fit between observed and modelled values; scores close to 1 indicate high accuracy (Yersaw & Chane, 2024).

2.5 Estimation of Potential Irrigation Requirement

In this study, water requirements for wheat cultivation under different climate scenarios were estimated using the FAO's CROPWAT model. Using particular inputs like climate and crop type, this model calculates crop water and irrigation requirements using the FAO Penman-Monteith method to estimate reference evapotranspiration (ETo). This model was modified for the current study to include bias-corrected climate data from three GCMs under two RCPs, RCP 4.5 and RCP 8.5, covering projected periods for the 2040s and 2070s. According to research like (Rahman et al., 2024), anticipated increases in irrigation demand brought on by climate change may help farmers better match water use to crop requirements, maximizing resources and possibly cutting expenses. Farmers can adopt precise water allocation strategies, such as modifying irrigation frequency during times of high demand and putting water-efficient techniques into practice, by anticipating these future irrigation needs. Additionally, CROPWAT has been extensively validated and used globally as a decision-support tool for figuring out regional irrigation needs, especially in scenarios with changing climates (Clarke et. al., 2001). Its reliability in precisely estimating crop water requirements is reinforced by the wide range of agricultural regions in which it finds use. For example, studies conducted in India and Nepal have validated the usefulness of CROPWAT by providing accurate estimates for rice and wheat irrigation under different climate scenarios (Agrawal et al., 2023). Studies conducted in Sub-Saharan Africa also show how well it models the water needs of staple crops like maize, indicating the model's adaptability to various climate zones (Solangi et al., 2022). In order to accurately model wheat requirements in Bangladesh's subtropical climate, these validations support CROPWAT's robustness. This study increases confidence in CROPWAT's accuracy for wheat projections under both historical and future climate scenarios by incorporating such well-documented validations. For this computation, the FAO-recommended Penman-Monteith method (Sen et al., 2019) was employed.

3. RESULTS AND DISCUSSION

3.1 Changes in Temperature and Precipitation During Wheat Season

3.1.1 Precipitation

Table 1: Monthly precipitation (mm) during the wheat season, Models for 2040s-4.5

Month	Baseline	BCC-CSM1-1-M_2040s_4.5	MIROC5_2040s_4.5	Average_2040s_4.5
November	10.52941	18.84369748	18.47703081	18.66036415
December	8.588235	1.502240896	3.1	2.301120448
January	5.529412	6.742016807	0.200840336	3.471428572
February	5.529412	1.911764706	17.1	9.505882353
March	69.41176	60.93333333	44.16666667	52.55
Total	99.588229	89.93305322	83.04453782	86.48879552

Table 2: Monthly precipitation (mm) during the wheat season, Models for 2040s-8.5

Month	Baseline	BCC-CSM1-1-M_2040s_8.5	MIROC5_2040s_8.5	Average_2040s_8.5
November	10.52941	11.45798319	5.586554622	8.522268906
December	8.588235	3.392717087	3.366	3.379358544
January	5.529412	7.094397759	4.353221289	5.723809524
February	5.529412	16.96890756	13.74509804	15.3570028
March	69.41176	58.53333333	44.26666667	51.4
Total	99.588229	97.44733893	71.31754062	84.38243977

Table 3: Monthly precipitation (mm) during the wheat season, Models for 2070s-4.5

Month	Baseline	BCC-CSM1-1-M_2070s_4.5	MIROC5_2070s_4.5	Average_2070s_4.5
November	10.52941	2.643697479	17.31036415	9.977030815
December	8.588235	1.502240896	1	1.251120448
January	5.529412	0.53	14.26666667	7.398333335
February	5.529412	10.67843137	14.83333333	12.75588235
March	69.41176	73.46666667	43.76666667	58.61666667
Total	99.588229	88.82103642	91.17703082	89.99903362

Table 4: Monthly precipitation (mm) during the wheat season, Models for 2070s-8.5

Month	Baseline	BCC-CSM1-1-M_2070s_8.5	MIROC5_2070s_8.5	Average_2070s_8.5
November	10.52941	4	12.08655462	8.04327731
December	8.588235	11.04061625	4.966666667	8.003641459
January	5.529412	5.238935574	7.086554622	6.162745098
February	5.529412	26.46890756	12.01176471	19.24033614
March	69.41176	70	43.76666667	56.88333334
Total	99.588229	116.7484594	79.91820729	98.33333334

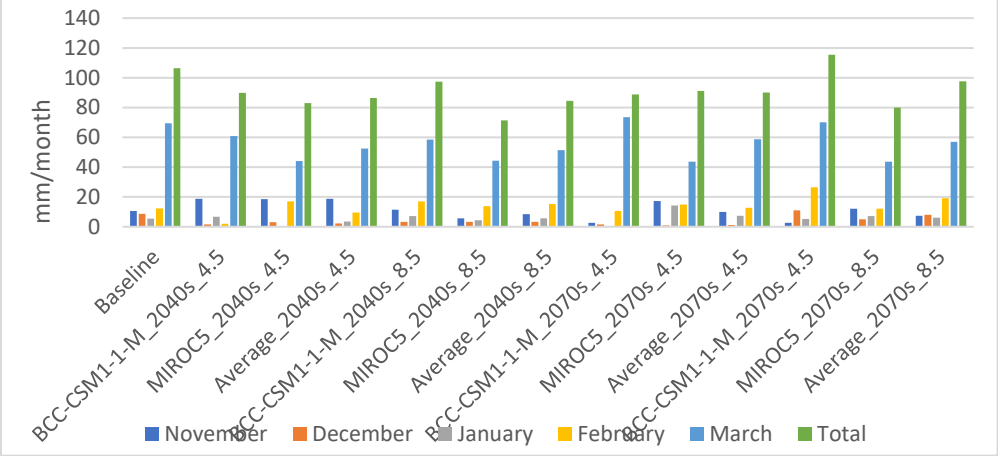

Fig 3: Projected percentage changes in rainfall during the Wheat season for the 2040s and 2070s, relative to the baseline period, based on various climate models under both RCP 4.5 and RCP 8.5 scenarios.

The precipitation trends differ between various scenarios and time periods, according to the bar chart. In the months of November, December, January and February, most scenarios show a discernible downward trend when comparing the baseline with the future projections for the 2040s and 2070s. Here, precipitation is expected to decline in the majority of future scenarios, especially in the early months (November to February) and overall yearly amounts. Water availability during the wheat-growing season may be significantly impacted by this reduction, which could have an impact on crop productivity and irrigation requirements.

3.1.2 Maximum Temperature (T_{max})

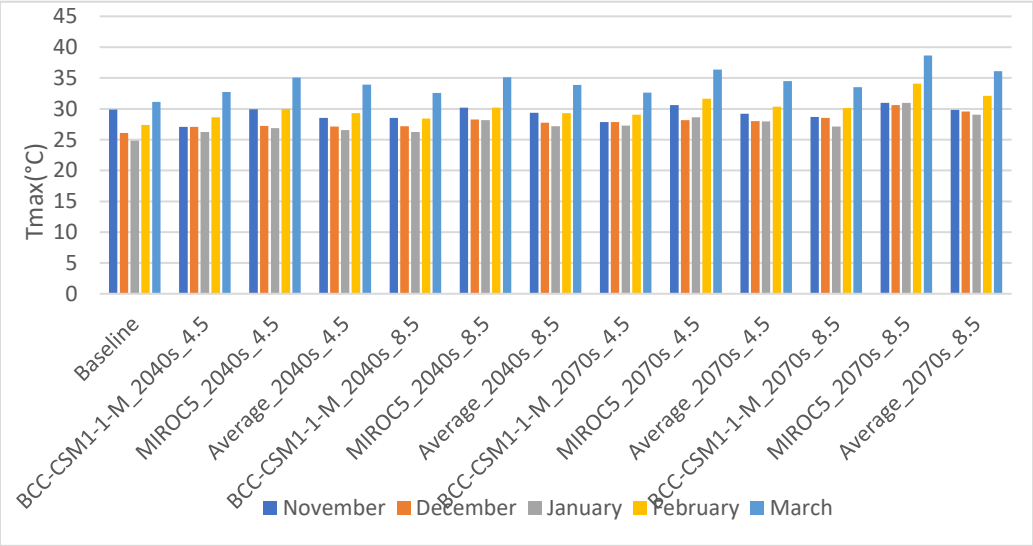

Fig 4: Projected maximum temperatures for the 2040s and 2070s, under the RCP 4.5 and RCP 8.5 scenarios, along with their baseline, during the Wheat growing season.

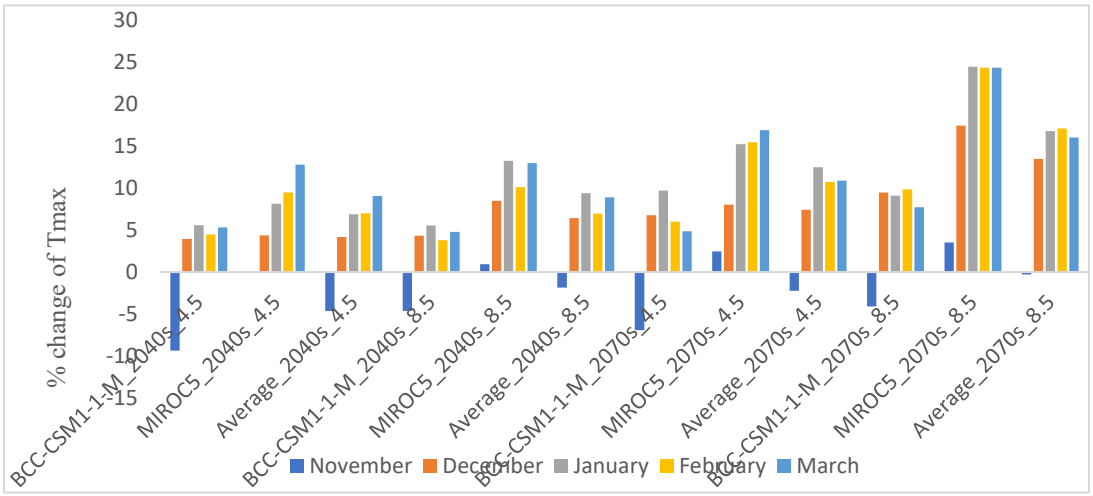

Fig. 5: Projected percentage changes in maximum temperature during the Wheat season for the 2040s and 2070s, relative to the baseline period, based on various climate models under both RCP 4.5 and RCP 8.5 scenarios.

A distinct upward trend in temperature can be seen in the bar chart that shows the maximum temperatures (Tmax, °C) for November, December, January, February, and March across the baseline and various climate scenarios. All months show an overall increase in maximum temperatures when comparing the baseline to future scenarios for the 2040s and 2070s. Over time, this increase becomes more noticeable, especially under the RCP 8.5 scenario, which denotes higher concentrations of

greenhouse gases. The highest Tmax values are consistently found in November and March, and the increase in these months under future scenarios is significantly greater than the baseline. Temperatures are rising in December, January, and February as well, but at a slower pace than in November and March.

3.1.3 Minimum Temperature (T_{min})

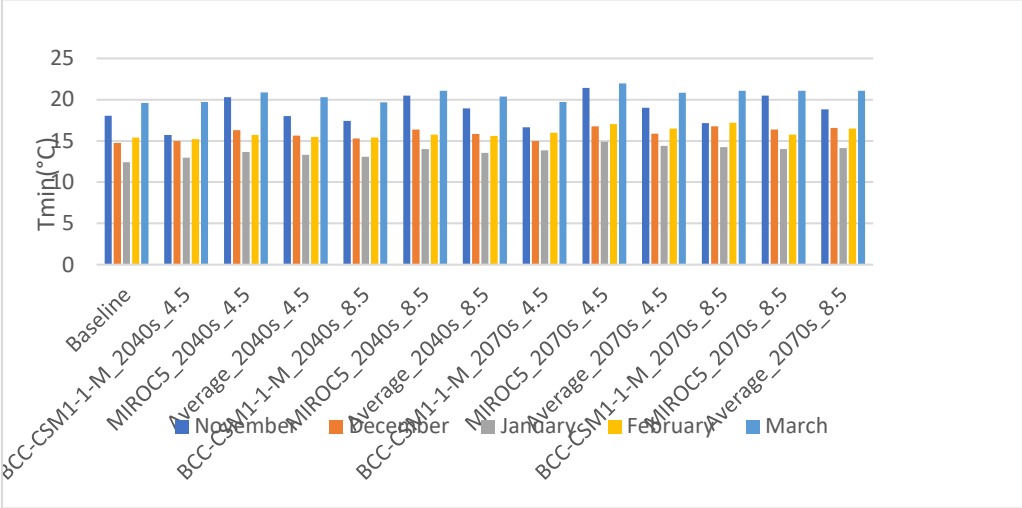

Fig. 6: Projected minimum temperatures for the 2040s and 2070s, under the RCP 4.5 and RCP 8.5 scenarios, along with their baseline, during the Wheat growing season.

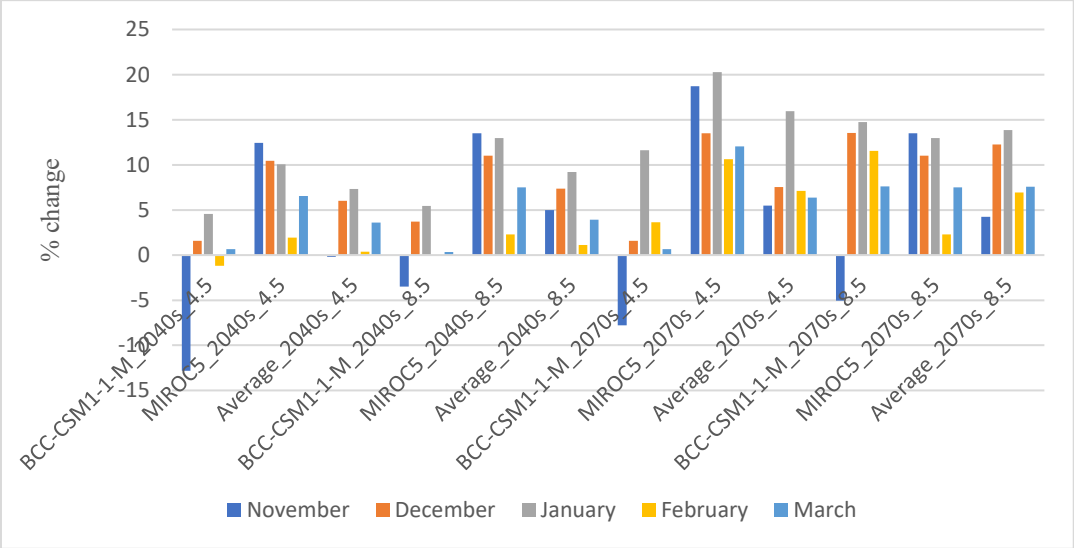

Fig. 7: Projected percentage changes in minimum temperature during the Wheat season for the 2040s and 2070s, relative to the baseline period, based on various climate models under both RCP 4.5 and RCP 8.5 scenarios.

The bar graph shows the calculated minimum temperatures (Tmin, °C) for November, December, January, February, and March under baseline and future climate scenarios for the 2040s and 2070s, using RCP 4.5 and RCP 8.5 pathways. All of the months show a consistent warming trend, according to the analysis. Both the 2040s and 2070s projections show a distinct rise in Tmin from November to March when comparing the baseline with future scenarios. This suggests a continuous warming trend since it shows a consistent increase in minimum temperatures across all months and scenarios. The highest Tmin values are consistently recorded in November and March, according to month-specific observations, with more noticeable increases under future scenarios. While the traditionally coldest

months of December, January, and February also show upward trends in Tmin, their rate of increase is marginally slower than that of November and March.

3.2 Changes in Reference Crop Evapotranspiration (ET_o) During Wheat Season

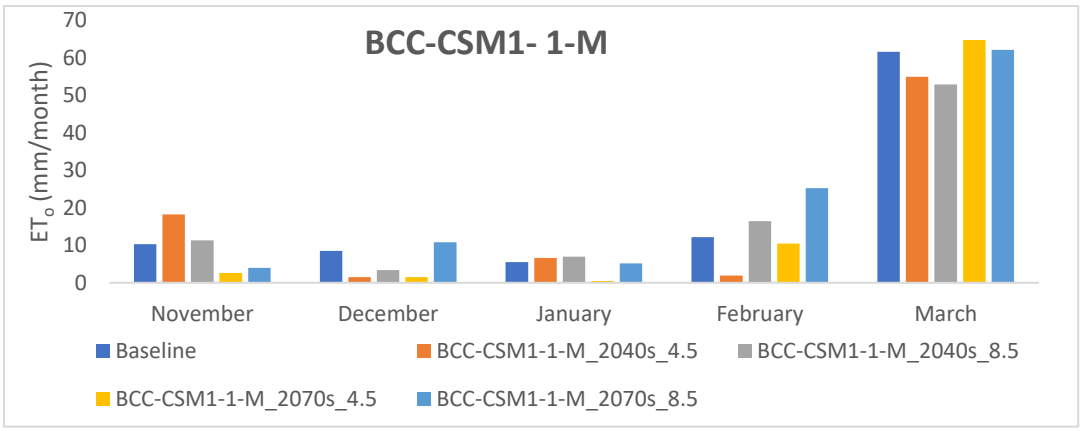

(a)

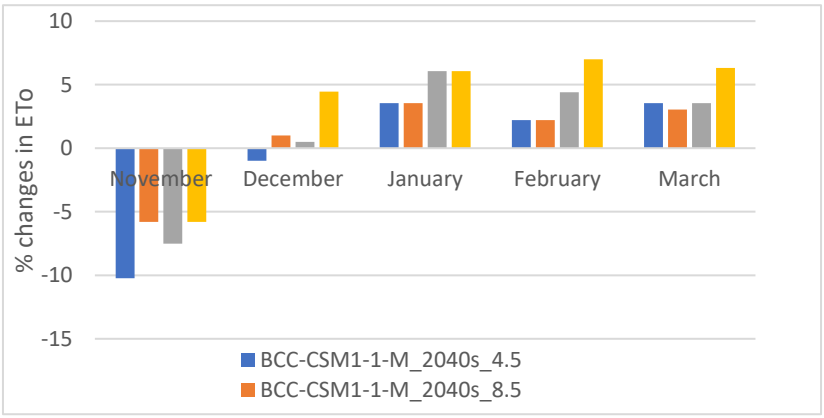

(b)

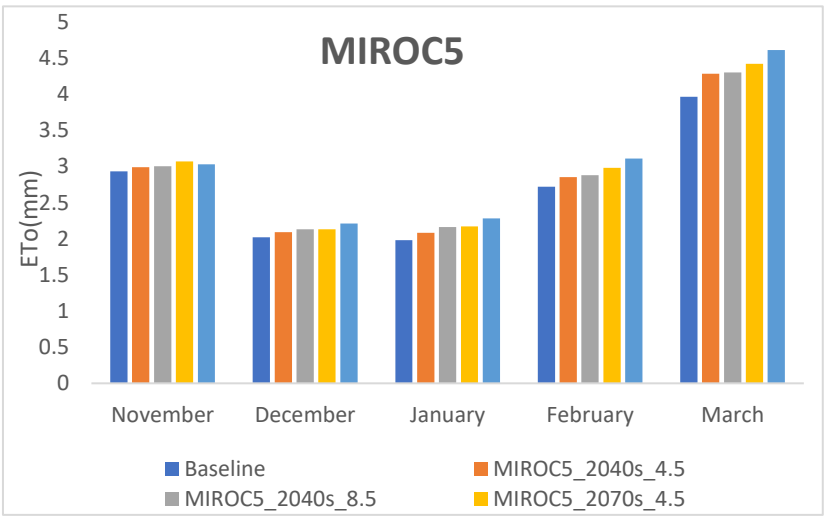

(c)

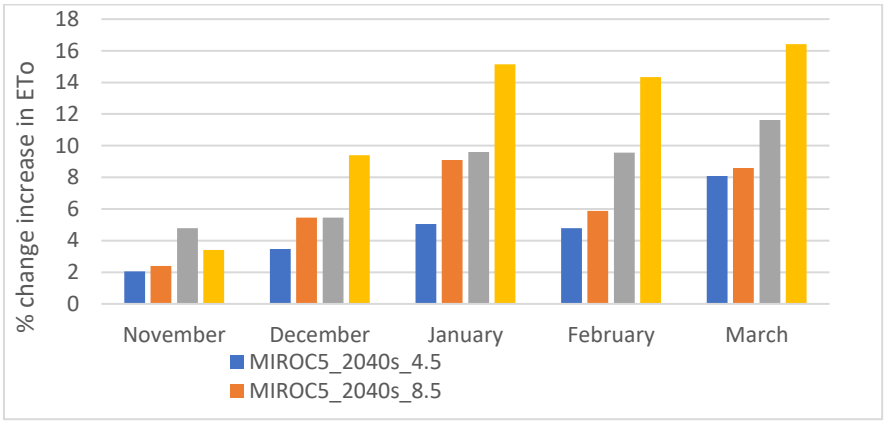

(d)

Fig 8(a-d): Monthly average reference crop evapotranspiration (ET_o) and its percentage change for the 2040s and 2070s compared to the baseline, projected under different GCMs for RCP 4.5 and RCP 8.5 scenarios during the Wheat growing season.

In comparison to the baseline, the reference evapotranspiration (ETo) increases by approximately +14.9% (RCP4.5, 2040s) and +16.4% (RCP8.5, 2040s), then rises to +18.6% (RCP4.5, 2070s) and +25.4% (RCP8.5, 2070s). Higher maximum and minimum temperatures, as well as variations in radiation and wind inputs used by the FAO Penman Monteith equation, all contribute to this pattern. In practical terms, an increase in ETo indicates that in future climates, the atmospheric demand for water from the crop soil system will be significantly higher; soil moisture will be drawn down more quickly, and crops will face more evaporative stress unless irrigation is modified. Even if rainfall stayed constant, these percentage increases directly translate into higher baseline irrigation requirements because ETo is the fundamental driver of crop water need calculations.

3.3 Projected Changes in Effective Rainfall, Potential Crop Water and Irrigation Requirement

3.3.1 Effective rainfall (ER)

With predicted changes of roughly −17.4% (RCP4.5, 2040s), −19.0% (RCP8.5, 2040s), −15.1% (RCP4.5, 2070s), and −6.4% (RCP8.5, 2070s), effective rainfall decreases in all scenarios. The decrease is due to both a change in the monthly distribution (less rain in November–February) and a decrease in the overall amount of rainfall for a large portion of the wheat season. Lower ER increases the percentage of crop water demand that must be satisfied by irrigation since it decreases the soil water contribution to the crop. The crop becomes more reliant on controlled water inputs as a result of this loss of effective rainfall, which increases vulnerability during sensitive crop stages.

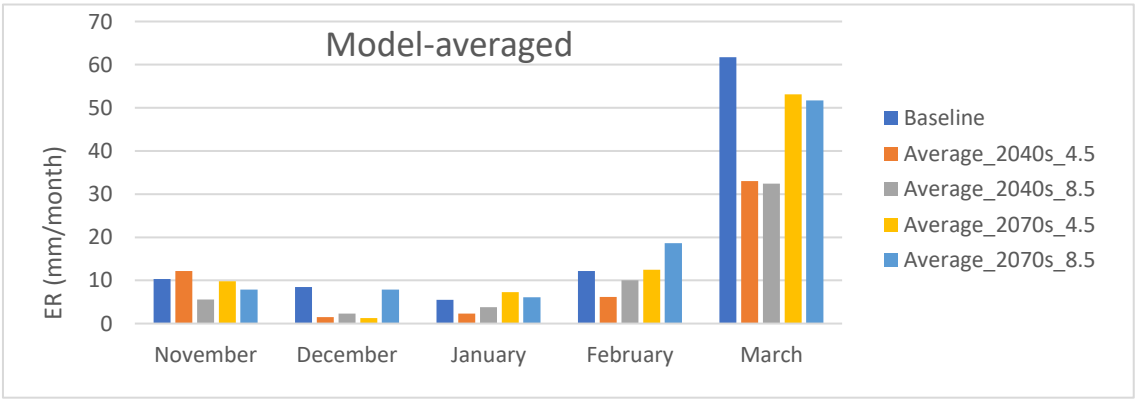

(a)

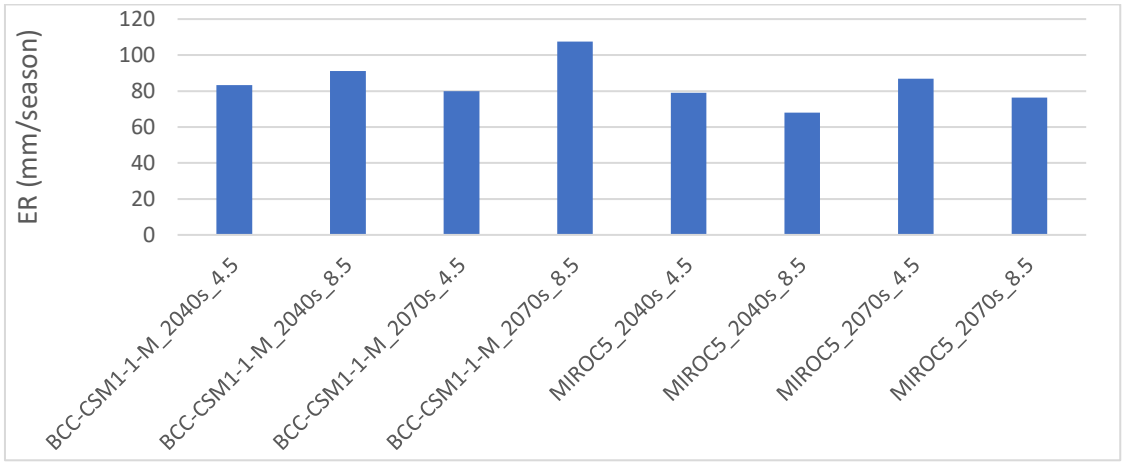

(b)

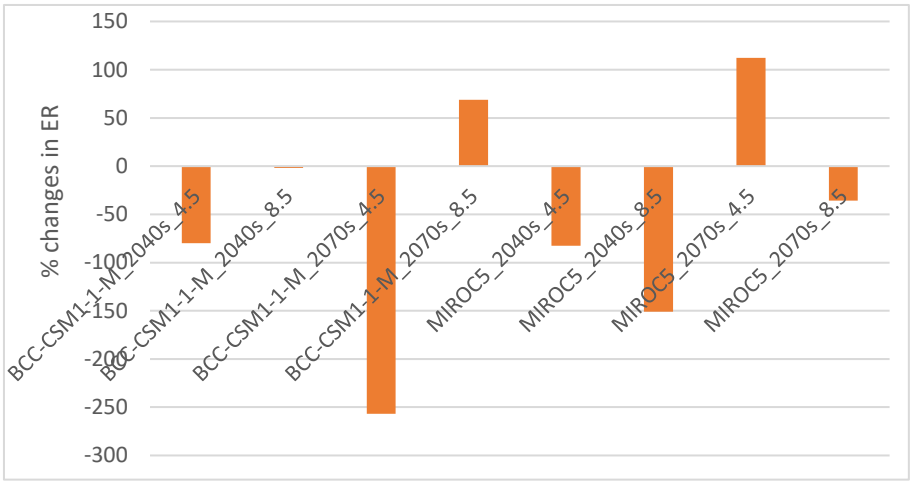

(c)

Fig. 9(a-c): Projected changes in effective rainfall (ER) during the Wheat season for the 2040s and 2070s, based on various climate models under both RCP 4.5 and RCP 8.5 scenarios.

3.3.2 Potential crop water requirement (PCWR)

With values around 86.5 mm (RCP4.5, 2040s), 84.4 mm (RCP8.5, 2040s), 90.0 mm (RCP4.5, 2070s), and 97.7 mm (RCP8.5, 2070s) displayed in the results table, projected PCWR increases slightly across scenarios. Increased ETo is the primary cause of the rise in PCWR; even in cases where rainfall continues in March, the increased atmospheric demand increases cumulative crop evapotranspiration. In summary, unless agronomic adjustments are made, crops will need more water throughout the growing season to attain the same growth and yield.

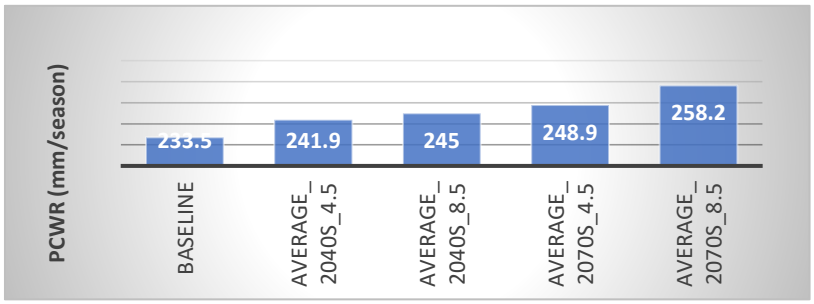

(a)

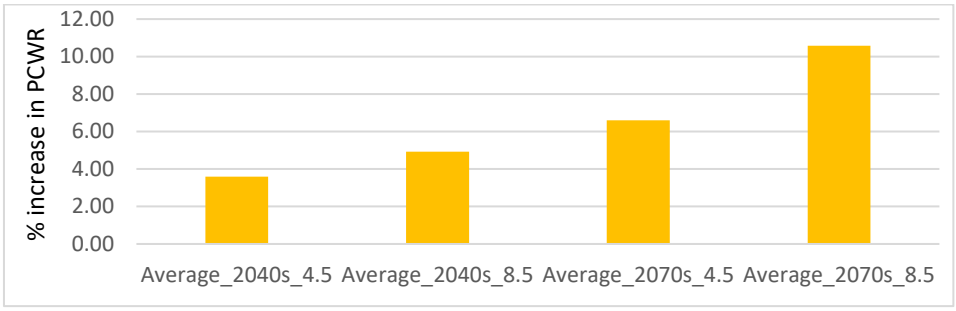

(b)

Fig. 10 (a, b): Projected changes in PCWR during the Wheat season for the 2040s and 2070s.

3.3.3 Potential irrigation requirement (PIR)

Future climates may require significantly more irrigation; the table shows PIR values close to 212 mm (RCP4.5, 2040s), 208 mm (RCP8.5, 2040s), 216 mm (RCP4.5, 2070s), and 212 mm (RCP8.5, 2070s). The consistent message is that irrigation demands stay at or above current levels and trend upward by mid- and late-century, despite some variation between models and scenarios. Higher PIR, when combined with less effective rainfall, necessitates the use of more irrigation water from surface or groundwater sources. This results in increased water abstraction, higher pumping costs, and possible resource stress, especially during dry months when river flows and shallow groundwater are at their lowest.

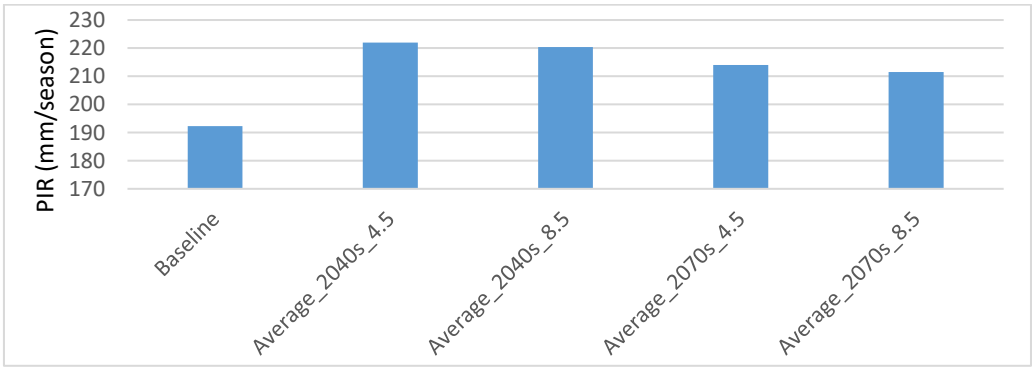

(a)

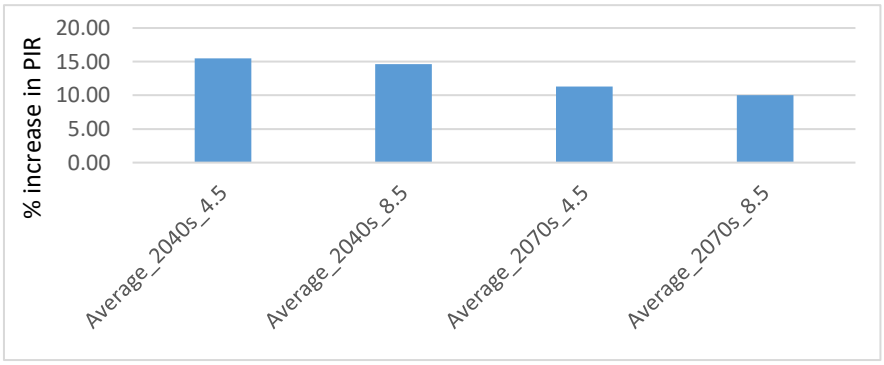

(b)

Fig. 11 (a, b): Projected changes in PIR during the Wheat season for the 2040s and 2070s.

4. CONCLUSION

This study used bias-corrected GCM outputs integrated with the FAO CROPWAT model to evaluate the effects of future climate change on wheat water requirements in Mymensingh, Bangladesh. Under RCP 4.5 and RCP 8.5 scenarios for the 2040s and 2070s, the analysis looked at anticipated changes in temperature, rainfall, reference evapotranspiration, effective rainfall and crop and irrigation water requirements. The findings indicate a steady increase in temperature, with seasonal Tmax and Tmin

rising by 1.2–2.6°C under RCP4.5 and up to 3.5–4.2°C under RCP8.5 by the 2070s. Higher atmospheric water demand is indicated by reference evapotranspiration, which rises by 14.9–18.6% (RCP4.5) and up to 25.4% (RCP8.5). Due mostly to less rainfall in November and February, the seasonal effective rainfall decreased by 6–19%, which reduced the amount of natural water available for crops. As a result, PIR increased from 234 mm to 248–259 mm and PCWR increased from 233 mm to 245–258 mm, indicating a 6–12% increase in irrigation demand. According to these results, the demand for irrigation for wheat in north-central Bangladesh will significantly rise due to climate change, placing more strain on the region's finite surface and groundwater supplies. Adaptive techniques like increased water storage, climate-resilient crop varieties, optimized planting schedules and improved irrigation efficiency will be crucial to sustaining future production.

Declaration of Use of AI: AI tools were used solely for language editing and clarity purposes. All scientific content and interpretations are the authors' own.

REFERENCES

Agrawal, A., Srivastava, P. K., Tripathi, V. K., Shrinivasa, D. J., Maurya, S., & Sharma, R. (2023). Future projections of crop water and irrigation water requirements using a bias-corrected regional climate model coupled with CROPWAT. Journal of Water and Climate Change, 14(4), 1147–1161. https://doi.org/10.2166/WCC.2023.349

Lamichhane, M., Phuyal, S., Mahato, R., Shrestha, A., Pudasaini, U., Lama, S. D., Chapagain, A. R., Mehan, S., & Neupane, D. (2024). Assessing Climate Change Impacts on Streamflow and Baseflow in the Karnali River Basin, Nepal: A CMIP6 Multi-Model Ensemble Approach Using SWAT and Web-Based Hydrograph Analysis Tool. Sustainability (Switzerland) , 16(8). https://doi.org/10.3390/SU16083262

D. Clarke, M. Smith, K. El-Askari, CropWat For Windows: User Guide, IHE, Oak Brook, IL, USA, 2001.https://www.researchgate.net/publication/312903822_CropWat_for_Windows_User_guide

Rahman, M. M., Chowdhury, M. M. I., Al Amran, M. I. U., Malik, K., Abubakar, I. R., Aina, Y. A., Hasan, M. A., Rahman, M. S., & Rahman, S. M. (2024). Impacts of climate change on food system security and sustainability in Bangladesh. Journal of Water and Climate Change, 15(5), 2162–2187. https://doi.org/10.2166/WCC.2024.631

Sen, R., Karim, N., Islam, M., Rahman, M., & Adham, A. (2019). Estimation of actual crop evapotranspiration and supplemental irrigation for Aman rice cultivation in the northern part of Bangladesh. Fundamental and Applied Agriculture, 0, 1. https://doi.org/10.5455/FAA.34264

Solangi, G. S., Shah, S. A., Alharbi, R. S., Panhwar, S., Keerio, H. A., Kim, T. W., Memon, J. A., & Bughio, A. D. (2022). Investigation of Irrigation Water Requirements for Major Crops Using CROPWAT Model Based on Climate Data. Water 2022, Vol. 14, Page 2578, 14(16), 2578. https://doi.org/10.3390/W14162578

Teutschbein, C., & Seibert, J. (2012). Bias correction of regional climate model simulations for hydrological climate-change impact studies: Review and evaluation of different methods. Journal of Hydrology, 456–457, 12–29. https://doi.org/10.1016/J.JHYDROL.2012.05.052

Watanabe, M., Suzuki, T., O'Ishi, R., Komuro, Y., Watanabe, S., Emori, S., Takemura, T., Chikira, M., Ogura, T., Sekiguchi, M., Takata, K., Yamazaki, D., Yokohata, T., Nozawa, T., Hasumi, H., Tatebe, H., & Kimoto, M. (2010). Improved Climate Simulation by MIROC5: Mean States, Variability, and Climate Sensitivity. Journal of Climate, 23(23), 6312–6335. https://doi.org/10.1175/2010JCLI3679.1

Wu, T., Song, L., Li, W., Wang, Z., Zhang, H., Xin, X., Zhang, Y., Zhang, L., Li, J., Wu, F., Liu, Y., Zhang, F., Shi, X., Chu, M., Zhang, J., Fang, Y., Wang, F., Lu, Y., Liu, X., … Zhou, M. (2014). An overview of BCC climate system model development and application for climate change studies. Journal of Meteorological Research 2014 28:1, 28(1), 34–56. https://doi.org/10.1007/S13351-014-3041-7

Yersaw, B. T., & Chane, M. B. (2024). Regional climate models and bias correction methods for rainfall-runoff modeling in Katar watershed, Ethiopia. Environmental Systems Research 2024 13:1, 13(1), 1–22. https://doi.org/10.1186/S40068-024-00340-Z